Jurnal Tribologi 41 (2024) 192-214

Analytical and computational sliding wear prediction of ultrahigh molecular weight polyethylene UHMWPE in block-on-ring (BOR) tribometer

Hussin M.S. [1*], Hamat S. [1], Kelly P.A. [2], Fernandez J. W. [3], Ramezani M. [4], Pranesh K. [5]

[1] Faculty of Mechanical Technology Engineering, Universiti Malaysia Perlis, 02600 Arau, Perlis, MALAYSIA.
[2] Department of Engineering Science, The University of Auckland, NEW ZEALAND.
[3] Auckland Bioengineering Institute, The University of Auckland, NEW ZEALAND.
[4] Department of Mechanical Engineering, Auckland University of Technology, NEW ZEALAND.
[5] SURGIONIX, 13E Paul Matthews Rd, Rosedale, Auckland, NEW ZEALAND.
[*]Corresponding author: mohdsabri@unimap.edu.my

KEYWORDS

Abrasion resistant steels
Scratch test
Worn surface
Work hardening
Wear

ABSTRACT

In knee joint replacement, wear of Ultrahigh Molecular Weight Polyethylene (UHMWPE) can be a significant factor in shortening the implant life span. With advancements in computational technology, virtual testing has become more reliable at a lower cost compared to physical testing. This paper evaluates the wear coefficient, k_D, from physical tests as a reliable predictor of wear volume in the computational method. The physical test run with a block-on-ring (BOR) configuration of UHMWPE on a steel counterface with 225N load for wear coefficient, k_D acquisition and 130N load for computational prediction validation using the same wear coefficient, k_D. The computational methodology involved the use of an Abaqus solver incorporating the UMESHMOTION subroutine to implement Archard's law. The maximum FEA result error was 14% in the 225N load test, and FEA prediction for the 130N load test was 17%. The results show that the wear coefficient,k_D produced by coupling UMESHMOTION in the computational method, is reliable for predicting wear volume in BOR physical test.

Received 26 October 2023; received in revised form 3 January 2024; accepted 12 April 2024.
To cite this article: Hussin et al., (2024). Analytical and computational sliding wear prediction of ultrahigh molecular weight polyethylene UHMWPE in block-on-ring (BOR) tribometer. Jurnal Tribologi 41, pp.192-214.

1.0 INTRODUCTION

Most of these joint replacements are necessitated by the damaging effects of osteoarthritis (OA). The goal of TKR is to reinstall the quality of life for the person who suffered from osteoarthritic knee pain. The incidence of osteoarthritis (OA) rapidly increases in patients over 50 years of age (Hooper, 2013). Knight et al. (2007) reported that, by 2030, the forecast demand in the United States for major TKR is projected to grow by 673% to 3.48 million procedures and that total knee revision (TKRe) is expected to raise by 601%, between 2005 and 2030.

Nowadays, a large number of knee replacement designs can be offered to the patient. In most of these designs, the articulating joint surfaces consist of a prosthetic material such as ultra–high molecular weight polyethylene (UHMWPE), titanium alloy or Cobalt chromium. However, wear of UHMWPE remains a large factor in restraining prosthetic life (Sharkey et al., 2002). In fact, younger patients' demands for an active lifestyle and longer prosthesis life expectancy have encouraged researchers to search for and explore new materials and designs. Furthermore, before human implantation, it is compulsory to pass the in-house preclinical evaluation and clinical tests. One of the critical evaluations which must be carried out is wear testing. Physical wear testing for joint replacements is time-consuming and very costly. This is because many months of data must be collected to mimic a large number of low-frequency walking gait cycles (Knight et al., 2007). For this reason, prosthetic bearing material evaluation has been developed comprehensively in conjunction with computer simulations incorporating physical and numerical wear models (McEwen et al., 2005).

The general engineering tribology research community developed and widely adopted standard physical wear tests to evaluate human prosthetic joints. In these procedures, a simple configuration of materials and surfaces is used to represent the articulating surfaces. Most researchers use the pin-on-disk (POD) arrangement as the bearing configuration. However, simple wear tests cannot comprehensively capture wear mechanisms seen in full joint simulators. The joint simulator assesses full geometrical shape in conjunction with bearing material arrangement. The complete simulator is, therefore, obviously, more complex and very much costlier than the simple testing (Haider & Garvin, 2008; Haider & Kaddick, 2011; Haider et al., 2012; Kurtz, 2009).

Numerous approaches have been developed to improve UHMWPE implant life expectancy (Kurtz, Muratoglu, Evans, & Edidin, 1999). In the earlier stages of testing, a material can be ranked (based on wear resistance) using simple POD test configurations. This can help produce good UHMWPE formulations for bearing materials before the materials are used and tested with more complicated and expensive equipment, for example in a full-wear joint simulator (J. Dumbleton, Shen, & Miller, 1974; J. H. Dumbleton, 1978; Wright, Dobbs, & Scales, 1982). Baykal et al. (2014) (Baykal et al., 2014) mention that, from the results of numerous tests, that multidirectional sliding POD is capable of ranking UHMWPE formulations concerning in vivo wear rates. However, the capability of the POD test to simulate realistically the true wear mechanism in vivo is still questioned. Ideally, test data should be produced repeatedly and compared across different research laboratories in order to develop a standardized test (Haider & Baykal, 2016).

With the POD wear-test configuration, ensuring that a consistent contact area and stress is achieved with the flat metal pin on the flat UHMWPE surface is not straightforward. This configuration produces edge effects, making it difficult to achieve a precise contact. This is also the case for pins with chamfer and curved edges. Since UHMWPE wear depends on the contact area and contact stress, edge effects associated with the flat metal pins will give rise to problems in determining the proper contact area and wear. However, Lewis (1998) suggest that a highly

convex or spherical configuration of metal pins should be used and that the approximate contact area can be estimated using the Hertzian contact theory. Although TKR mechanics models are more appropriately based on elastic foundation contact theory, such approximations have been validated with finite element analysis and also experimentally, using static pressure-sensitive film (Bartel, Bicknell, & Wright, 1986; Sanders, Lockard, Weisenburger, Haider, & Raeymaekers, 2016).

In order to replicate the pressure and contact stresses arising in a Total Knee Replacement (TKR), the selection of axial load and area of contact should be chosen carefully. This is because the compressive stresses seen in TKR have a wide range, from 2 to 50 MPa, depending on the particular TKR implant type (P. Walker, 2005). Many studies have been carried out on the relationship between contact pressure, area of contact, and the resulting UHMWPE wear behaviour (Mazzucco & Spector, 2003; Rostoker & Galante, 1979; Saikko, 2006). A number of researchers have proposed that static axial loading may result in higher wear compared to dynamic loading due to lubricant starvation (Charnley, 1976; J. H. Dumbleton, 1978; P. S. Walker, Blunn, & Lilley, 1996). On the other hand, Saikko and Kostamo (2011) reported that wear rates show no difference when using multiaxial POD experiments between dynamic loading and static loading. This difference in findings may be because of slight variations in the numerous factors involved, such as contact stress, applied load, velocities, surface topology, the flatness of pin, and kinematics, which all contribute to the wear result.

Although the wear rates obtained in POD experiments have been close to the clinically observed values, this does not assure that the wear mechanism experienced with the POD configuration is alike to that seen in vivo, due to the set-up simplifications (J. H. Dumbleton, 1978; McKellop, Clarke, Markolf, & Amstutz, 1978). Therefore, researchers have compared experimental samples from POD tests with retrieved implants, to assess whether the wear mechanisms are similar or not (Brown, Atkinson, Dowson, & Wright, 1976; J. H. Dumbleton, 1978). They found that, wear mechanism and wear coefficient are same order of magnitude.

Most researchers carry out the POD tests with Bovine serum (23 g/L) or Alpha calf serum (20 g/L) as lubricant (Lee & Pienkowski, 1998; Saikko, Calonius, & Keränen, 2001a; Saikko & Ahlroos, 1999b; Saikko, 2005; Turell, Friedlaender, Wang, Thornhill, & Bellare, 2005a). Both types of lubricants' viscosity are approximately 1.25 centipoises (cP) (Yadav, Shire, & Kalonia, 2011). These proteins are lubricants close to the knee joints' synovial fluid. This facilitates similar wear mechanisms as seen in in vivo during testing (Ahlroos, 2001; McKellop et al., 1978; P. S. Walker et al., 1996; Wright et al., 1982; Yao, Blanchet, Murphy, & Laurent, 2003). However, with the aforementioned lubricants, the wear factors obtained with unidirectional and reciprocating simple POD tests were one to three times smaller than that observed in retrieved Total Hip Replacements (THR) and Total Knee Replacements (TKR). Most probably, this phenomenon was due to simplifications made with geometry and other test environments (Bragdon et al., 2001; J. H. Dumbleton, 1978; Saikko & Ahlroos, 1999a; Turell, Friedlaender, Wang, Thornhill, & Bellare, 2005b; Wang et al., 1997).

Nonetheless, despite these test shortcomings, it has been possible to use POD testing to rank early bearing materials based on relative wear rates rather than exact wear rates (J. H. Dumbleton, 1978; McKellop et al., 1978; Wright et al., 1982). For example, in reciprocating POD testing comparing polytetrafluoroethylene (PTFE) and polyester to UHMWPE, results showed that wear rates in the former are substantially higher than that in UHMWPE, which is consistent with clinical outcomes (Mazzucco & Spector, 2006; McKellop et al., 1978).

Wear has customarily been quantified using wear coefficients or wear factors; these give the measured wear volume over a unit load over a unit sliding distance and are used in analytical wear models such as Archard's law wear model. Archard's law has been the gold standard in predicting wear material loss based on the relationship of sliding travelled distance and a magnitude of load (Barbour et al., 1995; Maxian et al., 1996; Fregly et al., 2005; Knight et al., 2007; Pal et al., 2008; Zhao et al., 2006, 2008). Archard's law considers the material surfaces to be rough to a certain extent, and that the deceptive contact area is larger than the actual contact area (Archard, 1953). This is because the real contact area at any point consists of touching asperities. Adhesion wear occurs where these asperities plough into softer materials and result in the removal of wear material/particles. Therefore, this model predicts more wear when a higher load is engaged.

The current study aims to valdiate a wear-testing Finite Element simulation model developed using the Abaqus software, using experimental wear testing. The simulation and testing configurations represent a simplified approximation of the articulating surfaces and geometry seen in a novel knee prosthesis assemblage. As discussed, many researchers carry out a POD test programs for knee prosthesis development; however, here the alternative Block-on-Ring (BOR) procedure is carried out, as the geometry is more similar to that of the knee prosthesis assemblage under study.

2.0 EXPERIMENTAL PROCEDURE

Experimentations procedure were conducted using a BOR tribometer. A magnitude of load was applied perpendicular to the sample test block, which has dimensions 12mm (width) x 12mm (height) x 18mm (length), as advice in the Ducom BOR machine test manual, model number TR-352. The test ring has a diameter of 35mm and 10mm width (Ducoms Instruments, 2016). The dimensions of the configuration are shown in Figure 1. As the ring rotates, a tangential friction force is transmitted across the surfaces; the detailed configuration is shown in Figure 2 and the machine arrangement is shown in Figure 3. It is presumed that the force is consistently distributed over the block. The ring rotated at 1000rpm and was run for 50,000 cycles per measurement interval. The machinery was inspected and tested by supplier Ducom Instrument Pvt Ltd to satisfy the ASTM G77, ASTM G137 standards.

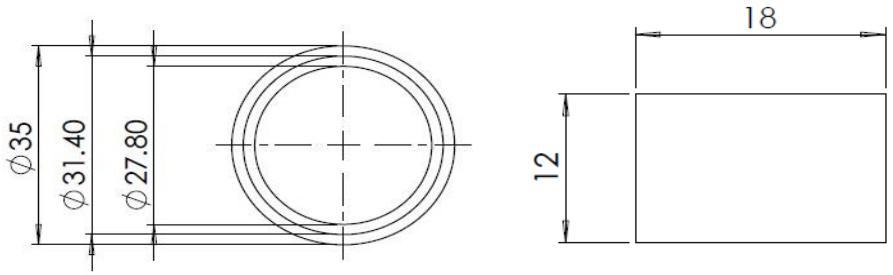

Figure 1: Block on ring configuration.

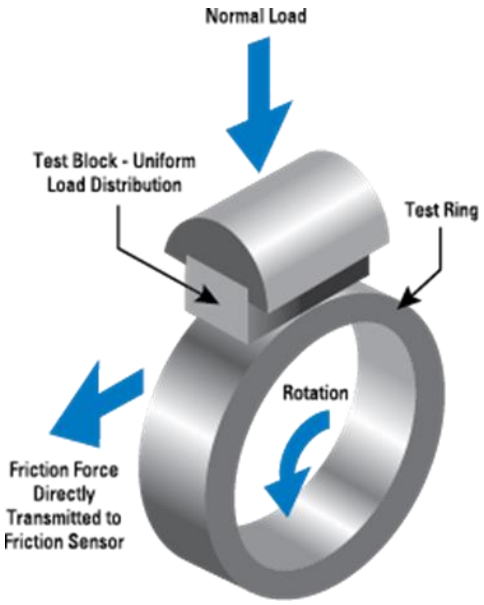

Figure 2: BOR specimen configuration.

Figure 3: BOR machine set up.

UHMWPE was used as the test block material; the material's specification, i.e. method of manufacture, material pureness, etc., is according ASTM D4020 standard. The material's hardness value, as used in some wear models, is listed by the supplier as 60-68 Shore D. For the test ring roller, E-52100 steel, hardened to 62-65HRc, is used. The ASTM standard for a Polyethylene-Metal combination, ASTM G-176 03, is used. Although this is not a commonly used combination of materials in standard knee prostheses, the main purpose of this test was to validate a numerical model that can predict wear (see further below).

Block and ring initial surface roughness were measured as this attribute plays a large role in wear. The ring was first polished so that its initial surface roughness was close to the surface roughness of a conventional femoral implant, i.e. in the range of 0.15-0.20 µm (Lee & Pienkowski, 1998; Saikko & Ahlroos, 1999b; Saikko, 2005; Turell et al., 2005a). Being the softer material, the

early roughness of the test block is not critical, as it will not affect wear significantly. The UHMWPE block and ring surface roughness measured using a Rtech 3D profilometer is depicted in Figures 4a and 4b.

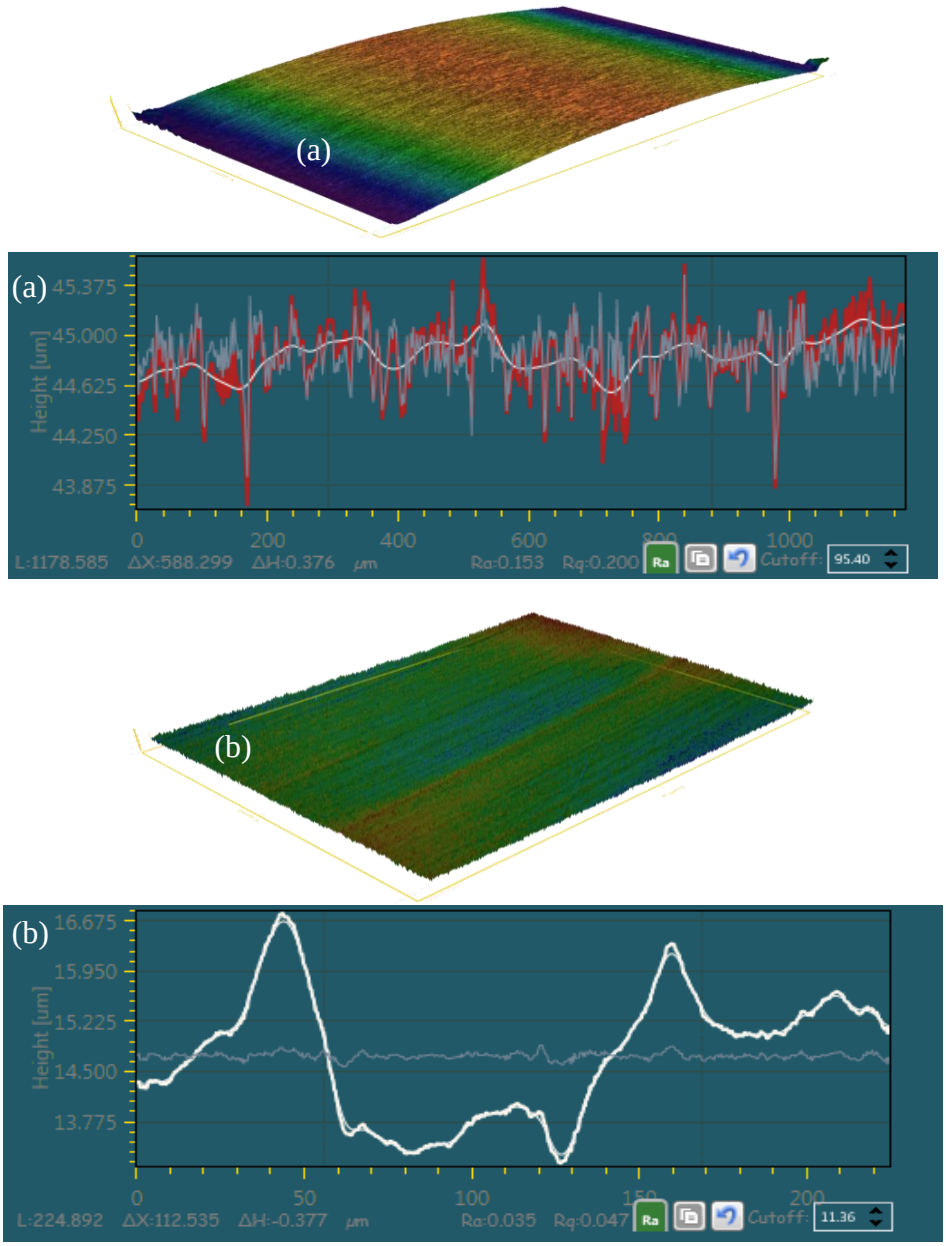

Figure 4: (a) ring surface roughness of approximately 0.153μm Ra; (b) UHMWPE block surface roughness of approximately 0.035 μm Ra.

The natural lubricant in the knee known as synovial fluid. Most researchers conduct wear testing, e.g. pin-on-disk implant testing, using Bovine serum (23 g/L) or Alpha calf serum (20 g/L) in their studies (Lee & Pienkowski, 1998; Saikko et al., 2001; Saikko & Ahlroos, 1999b; Saikko, 2005; Turell et al., 2005a). Both types of lubricants' viscosity are approximately 1.25 centipoises (cP) (Yadav et al., 2011). Due to a restraint of the BOR machinery, the lubricant chamber is incompatible to run with bovine serum.

The test had run with water a few times and observed some corrosive particles in the chamber. The corrosive particles came from the spindle. These corrosive particles affect the wear mechanism. This is because when the particles are immersed between two bodies caused excessive third-body wear, making the results not meaningful.

The tests were, therefore, carried out with a natural lubricant, soybean oil.(Note: According to the study by Cho and Murakami (Cho, Murakami, & Sawae, 2012), the wear rates seen in tests with bovine serum lubricant were lower than similar tests with distilled water as a lubricant.A lubricant is required to reduce the product of contact pressure and peripheral speed (PV) while running the test at 1000rpm. In order to avoid temperature effects at the contacting surfaces, a cooling water system is used to keep the chamber environment at ambient temperature.

One of the most important experimental parameters is the test load. In the wear model to be used (see below), the actual pressure-induced should not affect the wear rate coefficient. However, in reality, one would want the pressure in the test to be not too dissimilar to the pressure seen at real articulating surfaces to better ensure the results' reliability. The ASTM F732-00 is a standard for wear testing of material combinations in Total Joint Replacement suggests the force acting on axial axis is 225N so typical pressures on the contact surfaces should be around 3.54 MPa (ASTM F732-00, 2011). For the tests carried out in this study, two different loads will be used, as this will be a better test of robustness for the simulation models than if only one load value was used. Given the range of possible loads in the machine (100-500N), it was decided to run tests at 130N and 225N. The ear coefficient kD acquired from the BOR simulation with the 225 N load is used to predict wear at the load of 130N.

From previous studies, most researchers use steady-state wear-rates in the appropriate wear equations (Abdelbary, 2015). The combination of UHMWPE and metal used here typically gives rise to steady-state wear at around 3km sliding distance or after approximately 50 thousand cycles (Benabdallah, 1993; Friedrich & Schlarb, 2011; Saikko, Calonius, & Keränen, 2001b; Saikko, Vuorinen, & Revitzer, 2017; Saikko, 2017; Sawae, Murakami, Sawano, Noda, & Shimotoso, 2003; Turell et al., 2005b; Wannasri, Panin, Ivanova, Kornienko, & Piriyayon, 2009). For this reason, the tests are conducted to run for 200 000 rotations, more than adequate to reach steady-state. To acquire sufficient data points, the tests are run for a number of rotations, paused/stopped, samples are measured, and then resumed again. At least four instants are taken to measure wear volume: at 50k, 100k, 150k and 200k cycles, respectively. Each cycle-run takes approximately 50 minutes to complete. The wear coefficient, k_D, of Archard's law was determined by dividing the accumulated volume wear with sliding and axial force acting on the ring. Wear volume was measured from the average of 3 cross-sectional area along the wear scar, obtained using an RTech 3D profilometer as shown in Figure 5, and multiplied by the scar length.

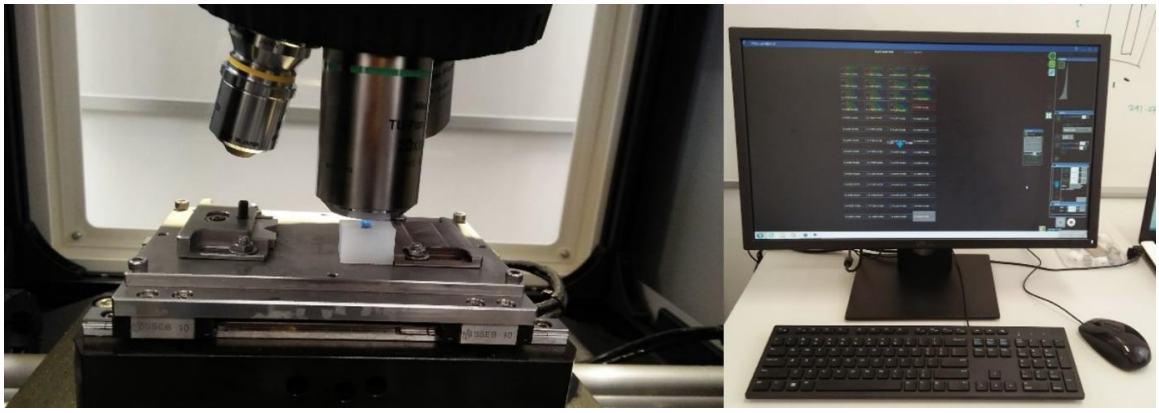

Figure 5: Wear-depth estimation using RTech 3D profilometer.

2.1 Semi-Analytic Wear Analysis

The computational model was verified using an available semi-analytic model of wear in BOR-type configurations (Zhao et al., 2008). Under the assumptions made in the computational model, the wear depth δ_{wear}, wear area A_{wear} and wear volume V_{wear} can be expressed as

$$\begin{aligned} \delta_{wear} &= R_w(1-\cos\theta') \\ A_{wear} &= 2R_c\, w \sin\theta \\ V_{wear} &= k_D\, F\, NS \end{aligned} \tag{1}$$

where *Rc* is the radius of the test ring, w the width of the test block, and *NS* the total sliding distance. The geometric parameters R_{wear}, θ,θ', were determined by solving a system of 3 non-linear equations in these 3 unknowns, as detailed in Appendix A.

2.2 Numerical Modeling

The geometrical configuration in the experimental test was constructed in CAD/CAE as in Figure 6 with a Commercial CAD package (SolidWorks®). The assembly was constructed to match exactly the experimental BOR set-up. The geometry was imported into ABAQUS as a 3D ACIS model (.sat file format). Material properties for the individual components, presented in Table 1, were assigned. The material properties such as density, Young's modulus, and Poisson's ratio were acquired from the material suppliers. The coefficient of friction is from the wear test on BOR tester machine. Both components were assigned linear elastic material properties. Need to note that, the polymeric materials exhibit actually viscoelastic mechanical behavior, however in these operating conditions the results are not change appreciably. An ALE adaptive meshing technique was adopted for the computational model (note that this method can lead to imprecise results for more complex material models such as hyper-elastic materials (Martinez, Canales, Izquierdo, Jimenez, & Martinez, 2012a)).By adopting ALE adaptive meshing method, uniformity of the mesh distribution around the worn area is maintained, when updating the new mesh and geometry at each iteration. This accurate geometry updating is crucial because this affects the contact pressure before and after wear evolution. Without ALE, excessive distortion can occur making the solution inaccurate.

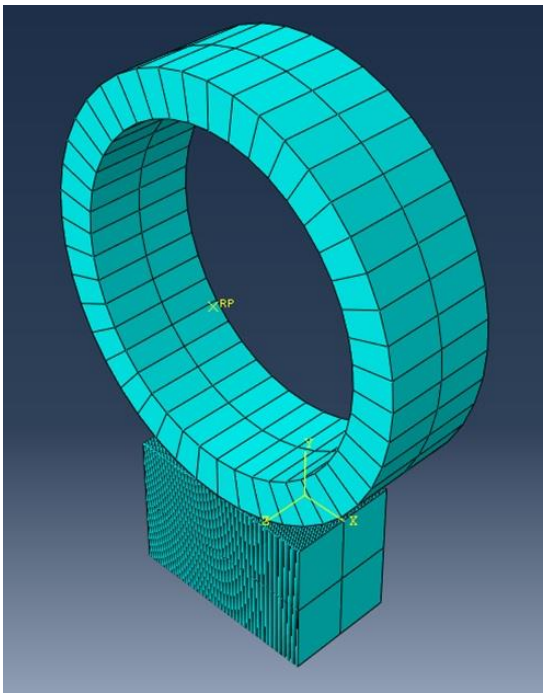

Figure 6: CAE Block on ring configuration.

Table 1 Material properties.

Material	Density [g/cm3]	Young Modulus [MPa]	Poisson Ratio	Coefficient of friction
UHMWPE	0.945	690	0.317	0.19
Steel	7.7	200000	0.3	

The simulation was divided into three steps. a) Compression loading. An axial load was applied to the center of the ring, and the UHMWPE block was fixed at the bottom surface using encastre boundary conditions. This gives the block compression loading on the UHMWPE block for static deformation. b) Compression loading with ring rotation. This step produces sliding and the contact pressures which produce the wear. The ring is rotated for 20 cycles as in the experiment. c) Unloading. This final step was carried out to evaluate wear volume and eliminate any deformation caused by the compression loading, which might affect UHMWPE block volume geometry.

The interaction between the contacts was defined in Abaqus as a surface-to-surface contact with the "Hard contact" property for pressure over closure. The "Hard contact" property can be found under normal behavior property. The "Hard contact" was chosen here because this minimizes the closure of the slave surface into the master surface at the particular contact without allowing tensile stress across the interfaces (Hibbitt, Karlsson, & Sorensen, 2001). The coefficient of friction (COF) was assigned a value of 0.19 using the tangential behaviour property. The COF was acquired from averaging the steady-state coefficient of friction during the experiment between the contact pairs, as given in Figure 7 and table 1. The boundary conditions were

assigned to the component with X-axis parallel to UHMWPE block top surface, Y-axis is perpendicular to the UHMWPE block top surface and the Z-axis is perpendicular to the UHMWPE block front surface. The ring was restricted from translating along the X-axis and Z-axis but allowed to rotate about the Z-axis during unidirectional sliding.

The solution was enhanced by applying reduced integration in elements to achieve faster computation. The entire UHMWPE block was discretized using 720 three-dimensional C3D8R 8-node linear brick elements (1629 nodes). In the UHMWPE block, enhanced hourglass control is deployed to provide course mesh accuracy improvement. For sensitivity studies of wear convergence, mesh sizes are varied to acquire a consistent wear and contact pressure so that dependence of mesh element size on the wear result is avoided.

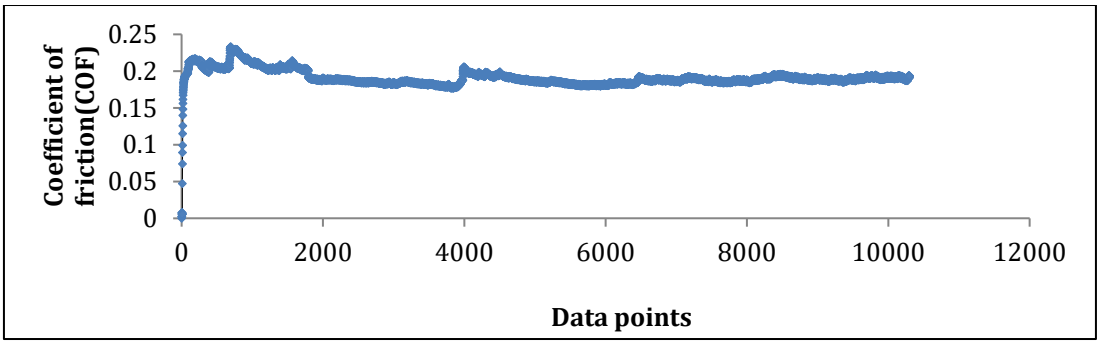

Figure 7: Coefficient of friction for the material configuration.

Adaptive mesh constraints were applied to the UHMWPE block geometry with 355 nodes in contact with the sliding ring contact surface. These constraints were deployed in order to prescribe independent mesh motion for nodes in adaptive domains (Hibbitt et al., 2001). From the experiments, wear was measured to occur only in the UHMWPE block. As such, element deletion was assigned to the UHMWPE block so as to enable material wear evolution.

The simulation was run for 20 cycles. Each cycle was divided into 100 increments and wear computational accumulated in every increment throughout the cycle. Every cycle is multiplied to 10 thousand cycles as described in the work of Netter et al (2015). This means 20 cycles in this simulation is equivalent to 200 thousand cycles in the experiment. The geometry changes and updates based on the contact pressure at any particular node. The simulation model does not account for speed as it involves a quasi-static analysis.

2.3 Description of Wear Subroutine

The general strategy used in the computational wear analysis is to solve the nonlinear contact problem and use the output contact pressure and sliding distance to compute wear. In the current study, Archard's wear law was implemented with the assumption that wear rate is a linear function of the contact pressure and sliding distance for the UHMWPE block in the steady-state region as acquired from the experiment:

$$q = \frac{k}{H} F.s \qquad (2)$$

where q is the wear volume of material loss from the softer material [mm3], H is the material hardness of the softer material [N/mm2], F is the axial load applied [N], s is the sliding distance and k is the dimensionless coefficient of wear. In generating the evolution of the wear profile, the strategy is to shift each contact node normal direction to the contact surface dependence to magnitude of the contact pressure. The displacement of a node shifted normally is the wear depth. Introducing a new wear para meter k_D, the dimensional coefficient of wear [mm^3/N.mm] representing wear volume per unit load per unit distance:

$$q = k_D \,.F.s \qquad (3)$$

$$k_D = \frac{q}{F.s} \qquad (4)$$

wear depth is obtained by dividing both sides of Eq3 by the incremental apparent contact area, ΔA,

$$\frac{q}{\Delta A} = k_D \,.\frac{F}{\Delta A}.s \qquad (5)$$

The wear depth increment, dh, can then be determined as

$$dh = k_D.p.ds \qquad (6)$$

where p is contact pressure [MPa] and ds is sliding distance increment [mm]. The total wear depth of contact surface is then

$$h = \int k_D \,.p.ds \qquad (7)$$

A user-defined Fortran UMESHMOTION subroutine was developed and utilized for wear computation. The UMESHMOTION utility is used to define motion nodes in an adaptive mesh constraint note set and to acquire nodes utility from Abaqus. This utility enables users to call and obtain nodes and elements data such as node location and coordinates and access local results at the nodes or elements (Hibbitt et al., 2001). The subroutine was developed to utilize Archard's law to modify and update the nodes at every iteration and generate the effect of wear. A flow chart giving an overview of the computational algorithm employed is given in Figure 10. All variables required to develop wear volume, such as contact pressure, tangential traction, slipping distance and area of contact, are collected from every node involved using the UMESHMOTION utility. Wear coefficient, k_D of the material configuration acquired from the BOR experiment, was used as an input parameter in the subroutine. To automate the data and geometry updating with the Abaqus FE package, Abaqus is linked to the Fortran compiler and Microsoft Video Studio. Node displacement is updated after each increment. At the end of the simulation, the last step involves unloading the UHMWPE block. As mentioned earlier, this final step is to make sure deformation effects do not influence the wear depth.

2.4 Mesh Convergence Study

A mesh convergence analysis was carried out by altering element size and mesh density to achieve consistent wear rates. A number of different model outputs could be examined in the mesh convergence study. Here, the critical contact pressure parameter results are given (since the wear volume is defined by wear depth, which depends directly on contact pressure). Results are shown in Figure 8. It can be seen that, when element size reaches 0.3mm (with 7293 elements), the contact pressure predicted appears steady and does not change perceptibly with a finer mesh. Therefore, in order to expedite the computational analysis without compromising the output accuracy, this element size and mesh has been chosen for the final FE model.

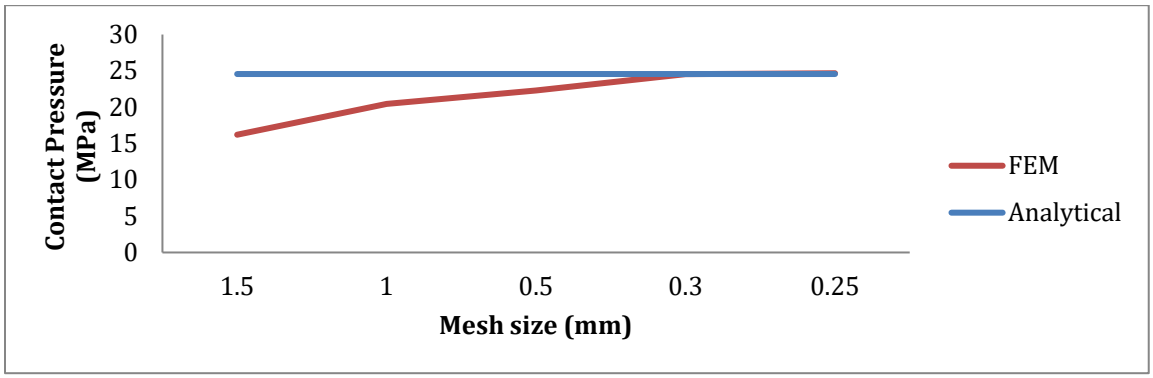

Figure 8: Mesh convergence study for the Finite Element Analysis.

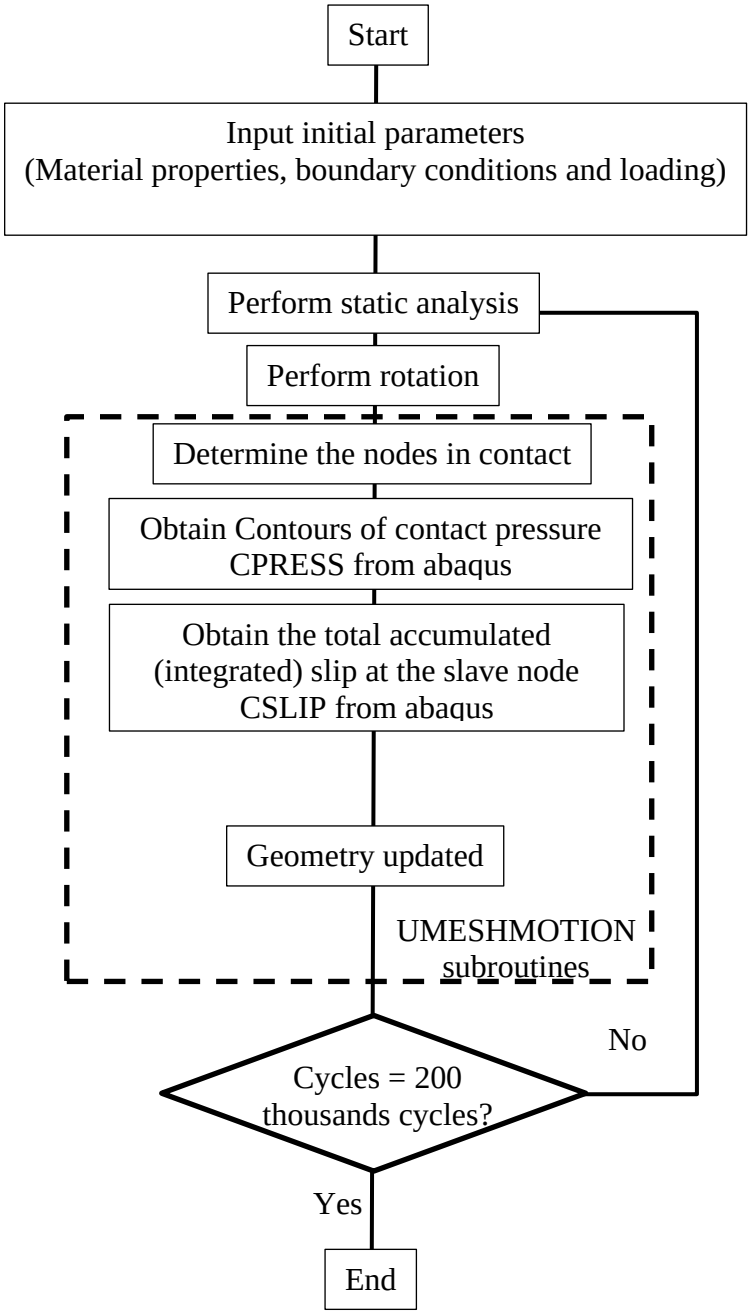

Figure 10: Finite Element Analysis wear simulation flow chart with incorperation of subroutines.

3.0 RESULTS AND DISCUSSION

Using the profilometer, the wear estimation is based on 3D images captured by an objective lens; 10X White Light Interferometry (WLI). The area for one image captured is 425 x 213μm2. Because the wear area sizes are more than one image, stitching methods can be done on multiple images captured and stitched together to produce one larger image. This apparatus feature is

perfect for analysis of a metallic component where the wear scar can be easily discerned, captured and estimated, as shown in Figure 9. For the UHMWPE blocks, the material needed to be first coated with a metal coating using Gold Sputter Coating so that it could be appropriately captured under the Rtech 3D profilometer, as shown in Figure 10. However, this coating may change the material surface significantly and make the block not amenable to testing and cycles.

To make the UHMWPE scarring discernible under the Rtech 3D profilometer without coating, a new objective lens type, 20X confocal objectives lens, was acquired. The 20X confocal lenses allowed the UHMWPE block to be measured accurately. However, the area captured was smaller than that of the 10X WLI objective lenses: 224 x 169 μm, making the stitching of UHMWPE images more complex and time-consuming, with more than 150 images needing to be captured for the wear scars in this experiment.

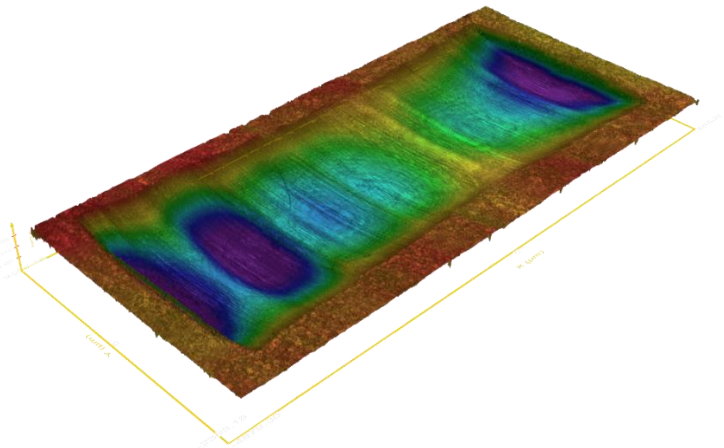

Figure 9: Wear volume estimation for the UHMWPE block using a 3D Rtect profilometer after coating with an atomic gold layer. The colours show the different surface depths; red is the lowest depth, followed by yellow, green, blue, dark blue and the deepest is violet.

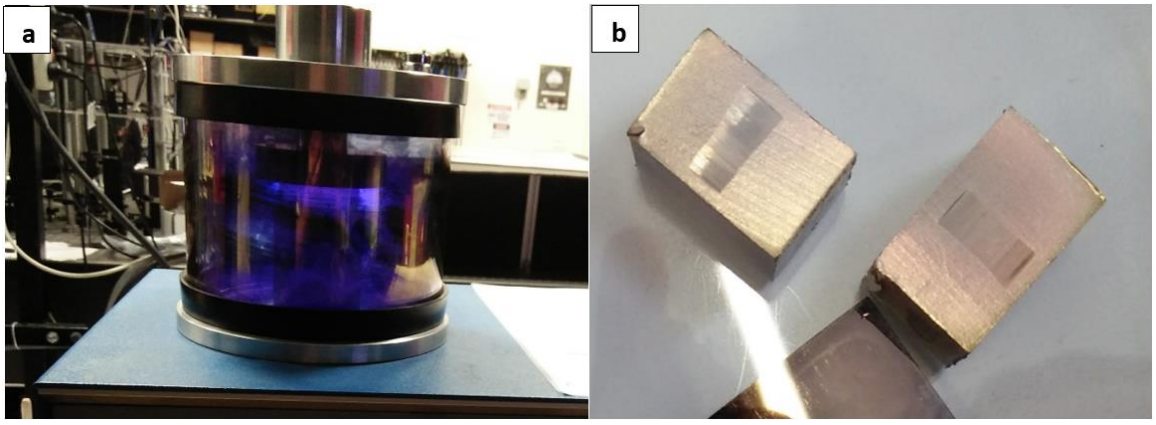

Figure 10: (a) a Gold Sputter Coating machine to coat the UHMWPE block with an atomic layer of gold; (b) an UHMWPE block after atomic gold coating.

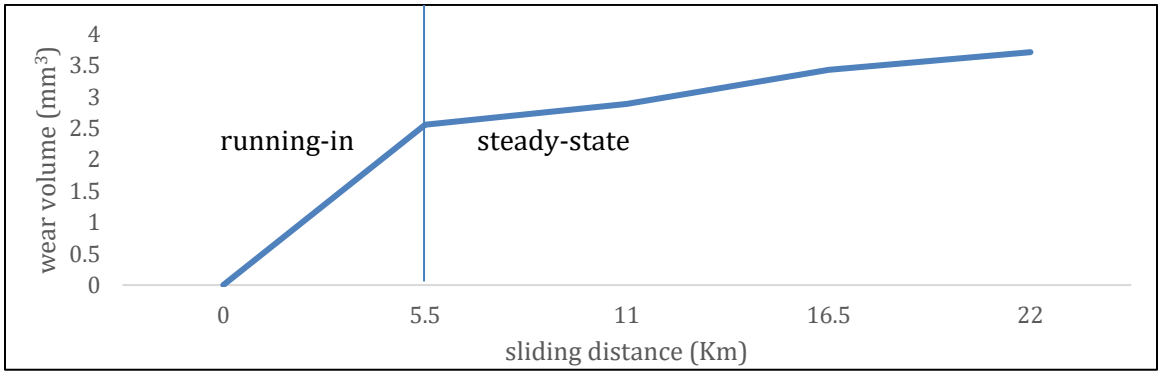

Figure 11: Volume of wear for block -on-Ring, Running-in, and steady state phases.

The experimental data acquired from the BOR wear tests are shown in Figure 11. The results show two distinct regions of UHMWPE wear: a) a "running in" region, where the wear rate is high, for the first 50,000 cycles. The wear rate is higher at the beginning of the sliding process due to the removal of surface impurities because of the manufacturing of the polymer specimen. Along the sliding process, asperities on UHMWPE surfaces (soft material surfaces) is building up and covering hard asperities on test ring surfaces and this makes the transition to the second phase (Abdelbary, 2015), b) a steady-state region where the wear increases consistently at an approximately constant wear-rate. Wear rate is lower than in the initial running-in stage because the UHMWPE asperities soften, and also the wear rate becomes steadier due to the lower surface roughness of the counterface (Abdelbary, 2015; Varenberg, 2013).

The final stages for UHMWPE wear are one where the wear rate increases rapidly again as a result of microscopic crack initiation and propagation due to surface fatigue, which leads to failure of a component (Hegadekatte, Huber, & Kraft, 2004); this region is not shown in Figure 11.

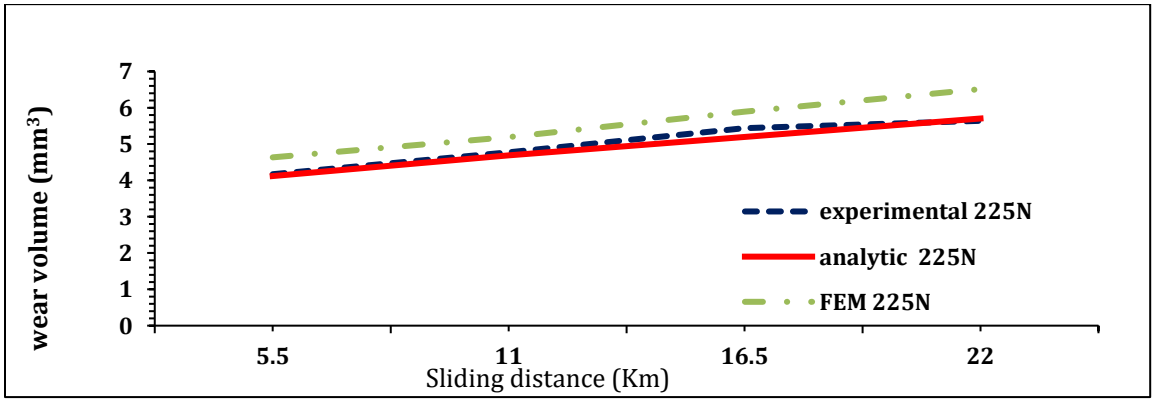

Figure 12: Wear volume for average experimental, analytical and FE simulations for 225 N.

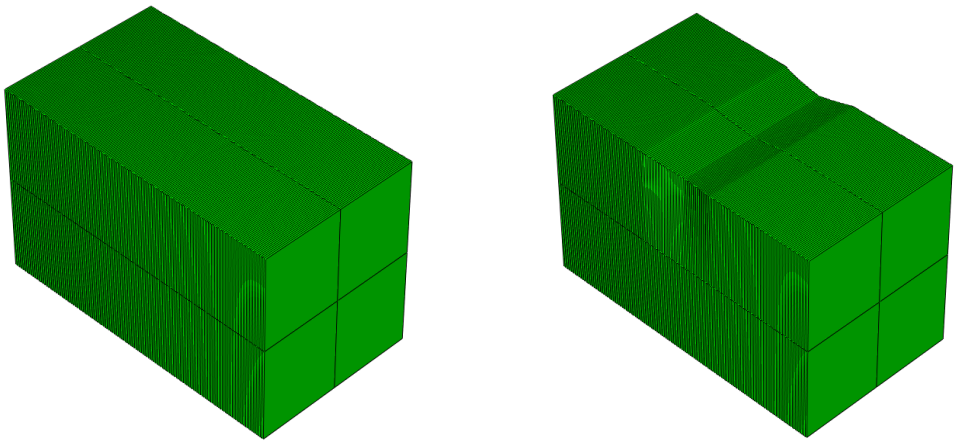

Figure 13: wear geometry in the FE model: initial and final.

The test was stopped after 200,000 cycles as the wear volume was seen to increase consistency and the wear coefficient, k_D, could be determined. The wear coefficient, k_D, is determined from the steady-state region; a k_D value of 4.1E-10 [mm^3/N.mm] was obtained. The slope at the steady-state region for the 225N experimental is 0.5075. The K factor was determined from Archard's law as in Eq4. This is evaluated from 4 steady-states data points from an average of 3 sets of experiment. As can be seen, there is good agreement between the analytical and experimental results.

This wear coefficient, k_D, is then used as an input for the wear simulation. The wear volume obtained from the Finite Element Analysis (FEA) and analytical estimation is plotted in Figure 12. The FEA model prediction is slightly higher than the experimental results. The maximum FEA prediction error is 14 %, occurring at the maximum of 200,000 cycles, which is within the bounds obtained by previous researchers (Bortoleto et al., 2013; Hegadekatte et al., 2004; Martinez, Canales, Izquierdo, Jimenez, & Martinez, 2012b; Podra & Andersson, 1999).

The wear geometry is depicted in Figure 13, which was captured after the final (200000th) cycle. The wear volume at this final stage was 6.5 mm3. For a better visualization, a magnification of 10 was prescribed to show the wear loss in Figure 13. The wear volume is extracted from the built-in Abaqus element volume function, VOL. During the simulation, the wear volume was extracted before and after each 50 thousand cycles interval. From Figure 13, note that the center wear depth is more than that at other nodes. This is because the center node experiences higher contact pressure. All the nodes experience contact pressure and sliding were move downwards according to Eq6. Then the model geometry was updated at every iteration by using the FORTRAN based subroutine linked with FE solver. As can be seen from the results, the developed FORTRAN subroutine was able to compute wear depth. Wear volume can be estimated from difference of initial and final volume.

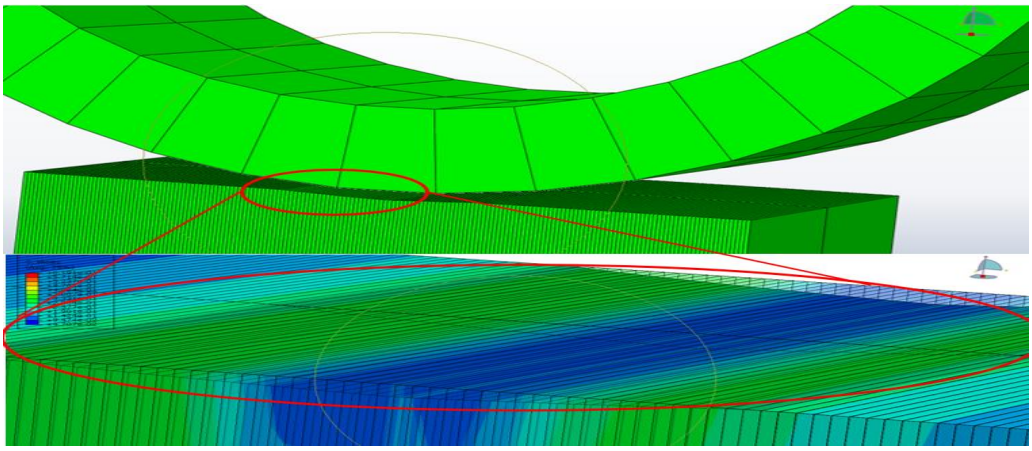

Figure 14: volume loss at final step.

3.1 Parametric Study

In order to evaluate the robustness of the model, the simulation was run for the same configuration, but with a different load. The objective was to predict the wear volume based on the wear coefficient, k_D acquired from the first model, in order to properly validate the simulation physical experiment. The wear volume predicted and obtained experimentally are compared in Figure 15. The results show that the FE model predicts the wear volume well.

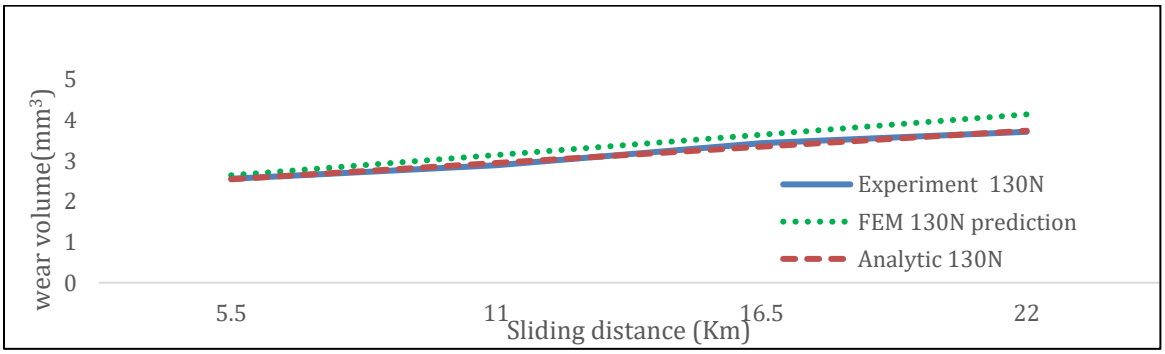

Figure 15: Wear volume for average experimental 130N, analytical and FE simulations prediction for 130 N load.

CONCLUSIONS

In this paper, sliding wear of a UHMWPE block was modeled successfully by developing a FORTRAN subroutine linked with ABAQUS. Material removal from the surface of the UHMWPE block in contact with steel counterface was defined by UMESHMOTION and Archard's wear law. ALE adaptive meshing method was implemented for geometry update due to surface ablation and despite some restrictions on material model selection, it maintained mesh stability and distortion control.

Results were in good agreement with experimental data obtained from the BOR wear tests. FE simulations tend to predict slightly higher wear rates as the BOR tests were conducted with

lubrication, while the lubrication was solely depended on the average coefficient of friction (COF) in the FEM model.

After ensuring the efficiency of the developed wear model, a parametric study was conducted to predict the same configuration with the different load to see the robustness of the simulation. The result shows that the wear prediction in different load is in a good agreement with the experiment. Thus, this showed that the FE model correlates well with the physical experiment. Therefore, the simulation strategies will be used in predicting wear in a novel distract knee in a future study.

ACKNOWLEDGEMENTS

The authors gratefully acknowledge the technical support of New Zealand National eScience Infrastructure (NeSI) team for the HPC access and the technical team from Auckland University Technology Tribology Lab.

REFERENCES

Abdelbary, A. (2015). Wear of polymers and composites Woodhead Publishing.

Ahlroos, T. (2001). Effect of lubricant on the wear of prosthetic joint materials Helsinki University of Technology.

Archard, J. (1953). Contact and rubbing of flat surfaces. Journal of Applied Physics, 24(8), 981-988.

Bartel, D. L., Bicknell, V., & Wright, T. (1986). The effect of conformity, thickness, and material on stresses in ultra-high molecular weight components for total joint replacement. Jbjs, 68(7), 1041-1051.

Baykal, D., Siskey, R., Haider, H., Saikko, V., Ahlroos, T., & Kurtz, S. (2014). Advances in tribological testing of artificial joint biomaterials using multidirectional pin-on-disk testers. Journal of the Mechanical Behavior of Biomedical Materials, 31, 117-134.

Benabdallah, S. (1993). The running‐in and steady‐state coefficient of friction of some engineering thermoplastics. Polymer Engineering & Science, 33(2), 70-74.

Bortoleto, E. M., Rovani, A. C., Seriacopi, V., Profito, F. J., Zachariadis, D. C., Machado, I. F., . . . Souza, R. M. d. (2013). Experimental and numerical analysis of dry contact in the pin on disc test. Wear, 301(1), 19-26.

Bragdon, C. R., O'Connor, D. O., Lowenstein, J. D., Jasty, M., Biggs, S. A., & Harris, W. H. (2001). A new pin-on-disk wear testing method for simulating wear of polyethylene on cobalt-chrome alloy in total hip arthroplasty. The Journal of Arthroplasty, 16(5), 658-665.

Brown, K., Atkinson, J., Dowson, D., & Wright, V. (1976). The wear of ultrahigh molecular weight polyethylene and a preliminary study of its relation to the in vivo behaviour of replacement hip joints. Wear, 40(2), 255-264.

Charnley, J. (1976). Wear of plastics materials in hip-joint. Plastics and Rubber, 1(2), 59-63.

Cho, C., Murakami, T., & Sawae, Y. (2012). Wear phenomena of ultra-high molecular weight polyethylene (UHMWPE) joints. Wear of orthopaedic implants and artificial joints (pp. 221-245) Elsevier.

Ducoms Instruments. (2016). Manual block on ring

Dumbleton, J. H. (1978). Wear and its measurement for joint prosthesis materials. Wear, 49(2), 297-326.

Dumbleton, J., Shen, C., & Miller, E. (1974). A study of the wear of some materials in connection with total hip replacement. Wear, 29(2), 163-171.

Friedrich, K., & Schlarb, A. K. (2011). Tribology of polymeric nanocomposites: Friction and wear of bulk materials and coatings Elsevier.

Haider, H., & Baykal, D. (2016). In Kurtz S. M. (Ed.), 30 - wear assessment of UHMWPE with pin-on-disc testing. Oxford: William Andrew Publishing.https://doi.org/10.1016/B978-0-323-35401-1.00030-2

Haider, H., & Garvin, K. (2008). Rotating platform versus fixed-bearing total knees: An in vitro study of wear. Clinical Orthopaedics and Related Research, 466(11), 2677.

Haider, H., & Kaddick, C. (2011). Wear of mobile bearing knees: Is it necessarily less? Journal of ASTM International, 9(2), 1-10.

Haider, H., Weisenburger, J. N., Kurtz, S. M., Rimnac, C. M., Freedman, J., Schroeder, D. W., & Garvin, K. L. (2012). Does vitamin E–Stabilized ultrahigh-molecular-weight polyethylene address concerns of cross-linked polyethylene in total knee arthroplasty? The Journal of Arthroplasty, 27(3), 461-469.

Hegadekatte, V., Huber, N., & Kraft, O. (2004). Finite element based simulation of dry sliding wear. Modelling and Simulation in Materials Science and Engineering, 13(1), 57.

Hibbitt, Karlsson, & Sorensen. (2001). ABAQUS/standard user's manual Hibbitt, Karlsson & Sorensen.

Hooper, G. (2013). The ageing population and the increasing demand for joint replacement. Nzmj, 126(1377), 1-2.

Knight, L. A., Pal, S., Coleman, J. C., Bronson, F., Haider, H., Levine, D. L., . . . Rullkoetter, P. J. (2007). Comparison of long-term numerical and experimental total knee replacement wear during simulated gait loading. Journal of Biomechanics, 40(7), 1550-1558. http://dx.doi.org/10.1016/j.jbiomech.2006.07.027

Kurtz, S. M. (2009). UHMWPE biomaterials handbook: Ultra high molecular weight polyethylene in total joint replacement and medical devices Academic Press.

Kurtz, S. M., Muratoglu, O. K., Evans, M., & Edidin, A. A. (1999). Advances in the processing, sterilization, and crosslinking of ultra-high molecular weight polyethylene for total joint arthroplasty. Biomaterials, 20(18), 1659-1688.

Lee, K., & Pienkowski, D. (1998). Viscoelastic recovery of creep-deformed ultra-high molecular weight polyethylene (UHMWPE). Characterization and properties of ultra-high molecular weight polyethylene () ASTM International.

Lewis, G. (1998). Contact stress at articular surfaces in total joint replacements. part II: Analytical and numerical methods. Bio-Medical Materials and Engineering, 8(5, 6), 259-278.

Martinez, F., Canales, M., Izquierdo, S., Jimenez, M., & Martinez, M. (2012a). Finite element implementation and validation of wear modelling in sliding polymer–metal contacts. Wear, 284, 52-64.

Martinez, F., Canales, M., Izquierdo, S., Jimenez, M., & Martinez, M. (2012b). Finite element implementation and validation of wear modelling in sliding polymer–metal contacts. Wear, 284, 52-64.

Mazzucco, D., & Spector, M. (2003). Effects of contact area and stress on the volumetric wear of ultrahigh molecular weight polyethylene. Wear, 254(5), 514-522.

Mazzucco, D., & Spector, M. (2006). Contact area as a critical determinant in the tribology of metal-on-polyethylene total joint arthroplasty. Journal of Tribology, 128(1), 113-121.

McEwen, H. M. J., Barnett, P. I., Bell, C. J., Farrar, R., Auger, D. D., Stone, M. H., & Fisher, J. (2005). The influence of design, materials and kinematics on the in vitro wear of total knee replacements. Journal of Biomechanics, 38(2), 357-365. http://dx.doi.org/10.1016/j.jbiomech.2004.02.015

McKellop, H., Clarke, I., Markolf, K., & Amstutz, H. (1978). Wear characteristics of UHMW polyethylene: A method for accurately measuring extremely low wear rates. Journal of Biomedical Materials Research Part A, 12(6), 895-927.

Netter, J., Hermida, J. C., D'Alessio, J., Kester, M., & D'Lima, D. D. (2015). Effect of polyethylene crosslinking and bearing design on wear of unicompartmental arthroplasty. The Journal of Arthroplasty, 30(8), 1430-1433. 10.1016/j.arth.2015.03.026 [doi]

Podra, P., & Andersson, S. (1999). Simulating sliding wear with finite element method. Tribology International, 32(2), 71-81.

Rostoker, W., & Galante, J. (1979). Contact pressure dependence of wear rates of ultra high molecular weight polyethylene. Journal of Biomedical Materials Research Part A, 13(6), 957-964.

Saikko, V. (2005). A hip wear simulator with 100 test stations. Proceedings of the Institution of Mechanical Engineers.Part H, Journal of Engineering in Medicine, 219(5), 309-318.

Saikko, V. (2006). Effect of contact pressure on wear and friction of ultra-high molecular weight polyethylene in multidirectional sliding. Proceedings of the Institution of Mechanical Engineers, Part H: Journal of Engineering in Medicine, 220(7), 723-731.

Saikko, V. (2017). Effect of contact area on the wear and friction of UHMWPE in circular translation pin-on-disk tests. Journal of Tribology, 139(6), 061606.

Saikko, V., & Ahlroos, T. (1999a). Type of motion and lubricant in wear simulation of polyethylene acetabular cup. Proceedings of the Institution of Mechanical Engineers, Part H: Journal of Engineering in Medicine, 213(4), 301-310.

Saikko, V., & Ahlroos, T. (1999b). Type of motion and lubricant in wear simulation of polyethylene acetabular cup. Proceedings of the Institution of Mechanical Engineers.Part H, Journal of Engineering in Medicine, 213(4), 301-310.

Saikko, V., & Kostamo, J. (2011). RandomPOD—A new method and device for advanced wear simulation of orthopaedic biomaterials. Journal of Biomechanics, 44(5), 810-814.

Saikko, V., Calonius, O., & Keränen, J. (2001a). Effect of counterface roughness on the wear of conventional and crosslinked ultrahigh molecular weight polyethylene studied with a multi‐directional motion pin‐on‐disk device. Journal of Biomedical Materials Research, 57(4), 506-512.

Saikko, V., Calonius, O., & Keränen, J. (2001b). Effect of counterface roughness on the wear of conventional and crosslinked ultrahigh molecular weight polyethylene studied with a multi‐directional motion pin‐on‐disk device. Journal of Biomedical Materials Research Part A, 57(4), 506-512.

Saikko, V., Vuorinen, V., & Revitzer, H. (2017). Effect of CoCr counterface roughness on the wear of UHMWPE in the noncyclic RandomPOD simulation. Journal of Tribology, 139(2), 021606.

Sanders, A. P., Lockard, C. A., Weisenburger, J. N., Haider, H., & Raeymaekers, B. (2016). Using a surrogate contact pair to evaluate polyethylene wear in prosthetic knee joints. Journal of Biomedical Materials Research Part B: Applied Biomaterials, 104(1), 133-140.

Sawae, Y., Murakami, T., Sawano, T., Noda, I., & Shimotoso, T. (2003). Surface characteristics and tribological behaviour of new zirconia ceramics for cementless knee joint prostheses. Tribology Series, 41, 263-271.

Sharkey, P. F., Hozack, W. J., Rothman, R. H., Shastri, S., & Jacoby, S. M. (2002). Why are total knee arthroplasties failing today? Clinical Orthopaedics and Related Research, 404, 7-13.
Turell, M., Friedlaender, G., Wang, A., Thornhill, T., & Bellare, A. (2005a). The effect of counterface roughness on the wear of UHMWPE for rectangular wear paths. Wear, 259(7), 984-991.
Turell, M., Friedlaender, G., Wang, A., Thornhill, T., & Bellare, A. (2005b). The effect of counterface roughness on the wear of UHMWPE for rectangular wear paths. Wear, 259(7), 984-991.
Varenberg, M. (2013). Towards a unified classification of wear. Friction, 1(4), 333-340.
Walker, P. (2005). Biomechanics of total knee replacement designs. Basic Orthopaedic Biomechanics and Mechano-Biology.3rd Ed.Philadelphia, PA: Lippincott, Williams and Wilkins, , 657-702.
Walker, P. S., Blunn, G. W., & Lilley, P. A. (1996). Wear testing of materials and surfaces for total knee replacement. Journal of Biomedical Materials Research Part A, 33(3), 159-175.
Wang, A., Polineni, V., Essner, A., Sokol, M., Sun, D., Stark, C., & Dumbleton, J. (1997). The significance of nonlinear motion in the wear screening of orthopaedic implant materials. Journal of Testing and Evaluation, 25(2), 239-245.
Wannasri, S., Panin, S. V., Ivanova, L., Kornienko, L., & Piriyayon, S. (2009). Increasing wear resistance of UHMWPE by mechanical activation and chemical modification combined with addition of nanofibers. Procedia Engineering, 1(1), 67-70.
Wright, K., Dobbs, H., & Scales, J. (1982). Wear studies on prosthetic materials using the pin-on-disc machine. Biomaterials, 3(1), 41-48.
Yadav, S., Shire, S. J., & Kalonia, D. S. (2011). Viscosity analysis of high concentration bovine serum albumin aqueous solutions. Pharmaceutical Research, 28(8), 1973-1983.
Yao, J. Q., Blanchet, T. A., Murphy, D. J., & Laurent, M. P. (2003). Effect of fluid absorption on the wear resistance of UHMWPE orthopedic bearing surfaces. Wear, 255(7), 1113-1120.
Zhao, D., Sakoda, H., Sawyer, W. G., Banks, S. A., & Fregly, B. J. (2008). Predicting knee replacement damage in a simulator machine using a computational model with a consistent wear factor. Journal of Biomechanical Engineering, 130(1), 011004.

APPENDIX A: SEMI-ANALYTIC WEAR ANALYSIS

An analytical solution for predicting wear volume V_{wear}, wear depth δ_{wear}, and wear area A_{wear} in the BOR experiment is given in Dong et al. (2008). In that analysis, the apparatus is modeled as a rigid cylinder of radius *Rc* pressed into and rotating on, a linear elastic plate of thickness *h* and width *w*, for *N* cycles. As depicted in Figure A1, the cylinder rotates around its longitudinal axis at a constant speed *S/Rc*. This rotation produces contact slip and each contact area will experience sliding at a constant speed S. The expression for V_{wear} is derived by integrating accumulated wear depth, δl along the wear zone area. The solutions are derived from this geometric configuration, Archard's wear law and the elastic foundation contact model.

$$V_{wear} = \int \delta_l dA \qquad \text{(EqA1)}$$

where *d*A is a differential area. In this equation, δ_l is found from the classical Archard's law,

$$\delta_l = k p_l N S \qquad \text{(EqA2)}$$

where k is the coefficient of friction, p_l is the contact pressure, and S is the cumulated sliding distance over N cycles. Substituting (Eq2) into (Eq1) gives:

$$V_{wear} = KNS \int p_l dA \qquad \text{(EqA3)}$$

Since $\int p_l dA$ is the axial force Fn acting on the cylinder, the volume wear can be expressed as:

$$V_{wear} = k F_n N S \qquad \text{(EqA4)}$$

To derive the wear depth δ_{wear}, and wear area A_{wear}, two assumptions need to be made: a) plate thickness h remains constant, and b) the wear scar formed on the plate is semi-cylindrical (Figure A1). By introducing the unknown radius Rw of the cylinder with unknown θ' angle, wear depth δ_{wear} is determined as the difference between the minimum worn contact and the flat surface of the block:

$$\delta_{wear} = R_w (1 - cos\theta') \qquad \text{(EqA5)}$$

In defining A_{wear}, an elastic foundation contact model is adopted since the model is defining the penetration of uniform contact surface. From this, A_{wear} can be expressed as:

$$A_{wear=}\, 2aw = 2R_c \, sin\, \theta w \qquad \text{(EqA6)}$$

By solving the above equations for the three unknowns, *Rw,* θ' and θ, δ_{wear}, and A_{wear} can be calculated. To complete the solution, three different geometric relationships are used. From figure A1, distance a is equal to of the half of wear zone *Rc* and wear zone *Rw*:

$$a = R_c \sin\theta' = R_w \sin\theta' \qquad 0 \le a \le R_c \qquad \text{(EqA7)}$$

The cylindrical wear volume is first determined from the geometric relationship between the cross-section and the cylinder block plane to get the total wear volume. The area shown in Figure A1 can be obtained by subtracting a triangular area from a circular sector area and then by multiplying the area to the plate width w:

$$V_{wear} = R_w^2 (\theta' - \sin\theta' \cos\theta') w \qquad \text{(EqA8)}$$

In order to develop elastic foundation contact to the V_{wear} equation, a new relation is made using the expression $F_n=\int \delta_l \, dA$ by defining p_l as below

$$p_l = \frac{(1-v)E}{(1+v)(1-2v)} \frac{(d_l - \delta_l)}{(h - \delta_l)} \approx C(d_l - \delta_l) \quad \text{(EqA9)}$$

It is assumed that the thickness of the layer h ≤ δ_l, the penetration of cylinder δ_l , and C is a constant for the material properties and thickness of the plate. With this expression for pl, the normal force can be written as

$$F_N = \int (d_l - \delta_l) dA = C(V_{geometry} - V_{wear}) \quad \text{(EqA10)}$$

where V_{wear} is known from (EqA4) and $V_{geometry}$ is given by an equation similar to (EqA8) for the intersection between the cylinder and unworn plane:

$$V_{geometry} = R_c^2(\theta - \sin\theta \cos\theta)w \quad \text{(EqA11)}$$

Substituting (EqA4) and (EqA11) into (EqA10) gives

$$F_n = C[R_c^2(\theta - \sin\theta \cos\theta)w - kNSF_n] \quad \text{(EqA12)}$$

Equations EqA7, EqA8 and EqA12 give three nonlinear equations in the three unknowns, Rw , θ' and θ. These equations can be solved using standard nonlinear root finding methods for any given number of cycles N.

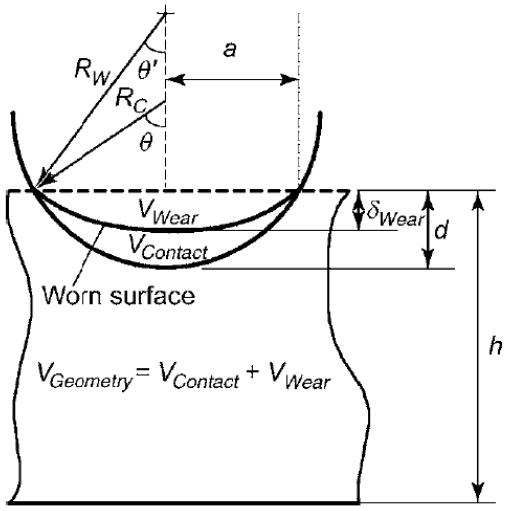

FigureA1: Schematics of cylinder on flat surface (Zhao et al., 2008).